Generalized Concatenated Encoded Gaussian Filtered CPM*†

Martin Bossert, Günther Haas, Armin Häutle, Hans Dieterich

Dept. of Information Technology, University of Ulm
e-mail: {boss|haas|armin|dieter}@it.e-technik.uni-ulm.de
WWW: http://it.e-technik.uni-ulm.de/ {boss|haas}

Sergo Shavgulidze

Dept. of Digital Communication Theory, Georgian Technical University,
e-mail: sergo_130@hotmail.com

Abstract — **In [1] it was described how generalized concatenated codes can be constructed on the basis of modulation with memory. In this paper we apply this idea to construct encoded (non-binary) Gaussian filtered CPM systems (GCPM). One possible application is EDGE (Enhanced Data Rates for GSM Evolution), a project of the ETSI (European Telecommunications Standards Institute), where higher data rates will be obtained by replacing the GMSK modulation (and coding) of the GSM system by some Higher Level Modulation (and appropriate coding). A GCPM construction has some obvious advantages compared to other proposed encoded modulation schemes such as encoded 8-PSK.**

I. Introduction

Continuous phase modulation (CPM) is known as a power and spectral efficient modulation scheme suitable for application in digital communication systems [2]. An important property of CPM is the constant envelope which avoids the necessity of expensive linear amplifiers.

With respect to the application EDGE, we consider M-ary Gaussian filtered CPM (GCPM) as a Higher Level Modulation in this work. This includes the popular binary case which is known as Gaussian minimum shift keying (GMSK) [3] and used in the GSM system. For GMSK, the alphabet size is $M = 2$ and the modulation index is $h = 1/2$. Thus GMSK can be seen as a subset of an M-ary GCPM scheme with $h = 1/M$. Therefore GCPM can be used for transmitting the GSM trainings sequence unchanged in EDGE as in the original GSM system without the need for two different modulators.

The traditional strategy is to construct encoded GMSK systems by matching binary convolutional codes and joint demodulation and decoding in the combined supertrellis by means of maximum-likelihood sequence detection based on the Viterbi algorithm [4]. In [5] an alternative two-stage receiver was also investigated which consisted of the separate demodulation of GMSK followed by the decoding of the convolutional code.

It was shown in [1] how generalized concatenated codes (GCC), or multilevel codes, can be constructed on the basis of inner modulation with memory, namely tamed frequency modulation. Thereby, an additive white Gaussian noise (AWGN) channel was assumed. We now apply this approach to non-binary GCPM signals. In other words, we consider GCC constructions with inner nested system of GCPM signals and outer binary convolutional codes with different error correcting capabilities. In this paper, we show results for encoded 4-ary and 8-ary GCPM over an AWGN channel. The latter is of special interest, because it directly could be compared to 8-PSK with Gaussian filtering and additional coding, which is the proposal for modulation in EDGE.

*This work was in part supported by the *Deutsche Forschungsgemeinschaft DFG* in Bonn, Germany.

†Revised Version (V5)

II. Generalized Concatenated Construction

A. Modulation

The usual description of a CPM signal can be found in [2]. In this paper we want to use a different approach, called tilted phase representation, which will be described very briefly in the following (for more details see [6]). It allows the decomposition of a CPM modulator into two parts: A linear continuous phase encoder (CPE) and a memoryless modulator (MM).

In general, a CPM signal can be described by

$$s(t,\underline{u}) = \sqrt{\frac{2E_s}{T_s}}\cos(2\pi f_1 t + \overline{\psi}(t,\underline{v}) + \varphi_0)$$

where E_s is the symbol energy, T_s is the symbol time, $f_1 = f_0 - h(M-1)/(2T_s)$ is the modified carrier frequency. The original carrier frequency is f_0 and φ_0 is a constant arbitrary phase offset. If we restrict the modulation index to be $h = 1/M$, the information-carrying physical tilted phase is given by

$$\begin{aligned}\overline{\psi}(\tau + nT_S, \underline{v}) \quad = \quad & \Big[2\pi h\Big[\sum_{i=0}^{n-L} v_i\Big]_{\bmod M} \\ & +4\pi h \sum_{i=0}^{L-1} v_{n-i} q(\tau + iT_s) \\ & + W(\tau)\Big]_{\bmod 2\pi}\end{aligned}$$

where $\underline{v} = v_0, v_1, \ldots, v_n, \ldots$ is a semi-infinite sequence of M-ary information symbols $v_n \in \{0, 1, \ldots, M-1\}$

and $W(\tau)$ is some information independent term, given exactly in [6]. The phase response is defined by $q(t) = \int_{-\infty}^{t} f(\tau)d\tau$ where $f(t)$ is the frequency response. For Gaussian filtered CPM it can be expressed as

$$f(t) = \frac{1}{2T_s}\left[Q\left(2\pi B_b \frac{t - T_s/2}{\sqrt{\ln 2}}\right) - Q\left(2\pi B_b \frac{t + T_s/2}{\sqrt{\ln 2}}\right)\right]$$

where $Q(t) = \int_t^\infty (1/\sqrt{2\pi})\exp(-\tau^2/2)d\tau$ and $B_b T_s$ is the normalized bandwidth. Since the frequency pulse has an infinite duration it is limited for practical reasons to L symbol intervals. The pulse length L can be considered as the memory of the modulator. In order to preserve the spectral characteristics, its value should be chosen large enough, so that $q(LT) = 1/2$ is satisfied.

One can directly see from the above representation that the tilted physical phase and the transmitted GCPM signal within some time interval $[nT_s, (n+1)T_s]$ only depends on the last L information symbols $v_n, \ldots, v_{n-L+1}$ and the sum

$$c_n = \left[\sum_{i=0}^{n-L} v_i\right]_{\bmod M}$$

which is an accumulation of all former information symbols. Using this fact, the GCPM modulator can be decomposed into a time-invariant memoryless modulator and a time-invariant continuous phase encoder with memory, which we call the GCPM encoder. It follows that the modulator state can be uniquely described by the L-tuple

$$(v_{n-1}, v_{n-2}, \ldots, v_{n-L+1}, c_n) \quad .$$

Therefore, M-ary GCPM with $h = 1/M$ can be represented by means of a trellis diagram which contains M^L nodes (states) at each tier and each node consists of M incoming and M outgoing branches. It can be seen from Fig. 1 that the conventional GCPM encoder model results in an encoder with feedback.

Fig. 2 shows the same modulator with an alternative realization of the continuous phase encoder. The adders in the right part of this CPE can also be realized in the memoryless modulator. Therefore it is possible to realize an equivalent feedback-free GCPM modulator with the same number of states, if the M-ary input symbols are differentially encoded by a conventional precoder with transfer function $T(D) = 1 - D$ (subtraction is carried out modulo M). This modulator is shown in Fig. 3. It realizes a modified GCPM scheme (MGCPM) with the same set of output signals and the same spectrum but with different mapping from information symbols to output signals compared to the conventional GCPM.

The input sequence of the GMSK modulator after the differential precoder is

$$v(D) = u(D)(1 - D)$$

where $u(D)$ is the D-transform of the precoder input sequence. The MGCPM continuous phase encoder including the precoder can be described by the generator matrix

$$\underline{G}(D) = (1, D, \ldots, D^L) \quad .$$

A state of the GCPM encoder trellis at a time n can be expressed by the L-tuple

$$\underline{\sigma}_n = (u_{n-L}, \ldots, u_{n-1}) \quad ,$$

and a branch in the trellis can be defined by

$$\underline{\gamma}_n = (u_{n-L}, \ldots, u_{n-1}, u_n) \quad .$$

In the following part of out paper only the MGCPM modulation is used.

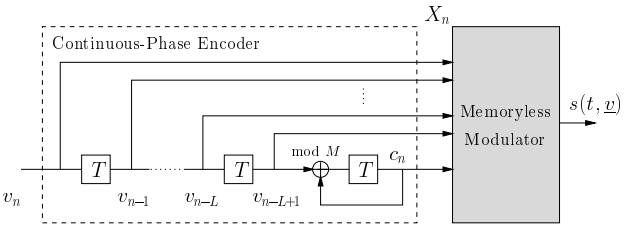

Fig. 1: Decomposition of an L-response GCPM modulator.

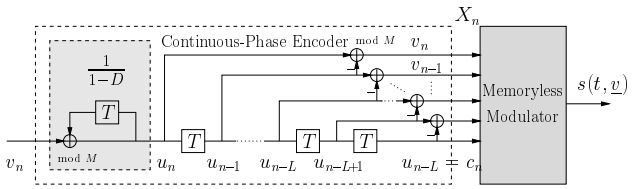

Fig. 2: Decomposition of an L-response GCPM modulator with alternative realization of CPE.

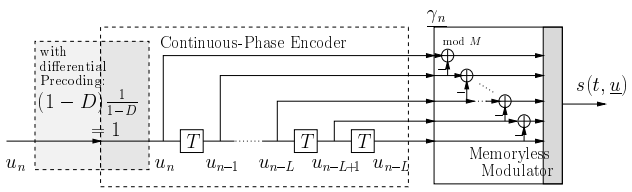

Fig. 3: Modified L-response GCPM modulator (MGCPM).

B. Partitioning with Scrambler

For the construction of a GCC scheme, a partitioning method is needed which partitions the inner system (here MGCPM modulation) into nested subsystems with improved characteristics. We apply the partitioning method via scrambler as presented in [1], [7], and [8] to increase the Euclidean distance in each partitioning step. In the following the main idea is shortly described. For more details see [1], [7] and [8].

Consider the trellis diagram of MGCPM where each path in the trellis described by a sequence of transitions corresponds to a transmitted MGCPM signal. In order to obtain a subsystem of MGCPM signals, a path puncturing method can be considered where within the trellis, paths are deleted by puncturing certain transitions $\underline{\gamma}_n$ in the trellis by periodically fixing certain bits in the information sequence. The trellis with the reduced set of paths gives the subsystem.

The aim is to reach in all subsystems a higher Euclidian distance compared to the original set of signals. To achieve this goal, distances between all possible pairs of signals in the original set have to be calculated. Then, if it is possible, the signals of pairs with small distance have to be put into two different subsets by means of partitioning. (In case of partitioning of linear convolutional codes, it is sufficient to regard always only the linear subcode and its free distance (see [9] and [10]). That is not sufficient for nonlinear case that includes the partitioning of MGCPM.)

Table 1: Inverse Scrambler Matrices for 4-ary and 8-ary MGCPM with $B_bT_s = 0.3$, $h = 1/M$ and $L = 2$

.

M	Scr.	inv. Scrambler	j	$d^{2,(j)}$	$\delta^{2,(j)}$
4	I_2	$\begin{pmatrix} 1 & 0 \\ 0 & 1 \end{pmatrix}$	1	1.09	
			2	3.63	
	C_2	$\begin{pmatrix} 1+D^2 & D \\ D & 1 \end{pmatrix}$	1	1.09	
			2	5.11	
	C_4	$\begin{pmatrix} 1 & 1+D & 0 & 0 \\ 0 & 0 & 1 & 1 \\ 1+D & D & D & 1 \\ 0 & D & 1 & 0 \end{pmatrix}$	1	1.09	
			2	1.20	
			3	3.63	
			4	9.68	
8	I_3	$\begin{pmatrix} 1 & 0 & 0 \\ 0 & 1 & 0 \\ 0 & 0 & 1 \end{pmatrix}$	1	0.28	0.42
			2	1.09	1.63
			3	3.63	5.44
	C_3	$\begin{pmatrix} 1 & 0 & 0 \\ 0 & 1+D^2 & D \\ 0 & D & 1 \end{pmatrix}$	1	0.28	0.42
			2	1.09	1.63
			3	5.11	7.66

In most cases, using the input sequence directly for the puncturing (we call it arbitrary partitioning) does not consistently improve the distances within the subsets. In order to find the best path puncturing, the mapping of the information sequences to the signals is changed by a scrambler. The cascade of this scrambler and the original MGCPM encoder can be considered as an equivalent MGCPM encoder.

A systematic computer search was performed to find the best scrambler matrices C_m for 4-ary MGCPM with $m = 2, 4$ partitioning levels. The results are listed in Table 1 in form of the inverse Scramblers where $d^{2,(j)}$ is the squared free Euclidean distance and $\delta^{2,(j)}$ is the normalized squared free Euclidean distance in the MGCPM (sub)systems of step j, $j = 1, 2, \ldots, m$.

For 8-ary MGCPM with m =3 partitioning levels, the best scrambler that could be found up to now is identical to the unity matrix (I_3). Although using I_3 is equal to arbitrary partitioning (without a scrambler), increased distances are obtained in the subsets.

A second scrambler C_3 for 3-level partitioning of 8-ary MGCPM can be directly constructed using the scrambler $C2$ for 4-ary MGCPM. This can be done by simple expansion of C_2^{-1}

$$C_3^{-1} = \begin{pmatrix} 1 & (0,0) \\ (0,0)^T & C_2^{-1} \end{pmatrix} \quad ,$$

where the first subset of 8-MGCPM can be regarded as 4-MGCPM having the same distance properties. Therefore, one gets the same squared Euclidean distance $d^{2,(3)}_{8-MGCPM} = d^{2,(3)}_{4-MGCPM} = 5.11$ in the third partitioning step as in the second partitioning step of 4-ary MGCPM when C_2 is used. This scrambler was not used in the simulations due to the following reason: The changed mapping realized by the second row of C_3^{-1}, which results in the bigger distance gain in the third partitioning step, also leads to a small loss in the bit error performance of the second level, which in its turn leads to a loss in overall performance.

C. Generalized Concatenated MCPM Scheme

Now we are able to construct a generalized concatenated code using the partitioning of the inner code (MGCPM). Since each of the m subsystems of signals should have different distance characteristics, we use m outer convolutional codes with error-correcting capabilities adapted to the corresponding inner subsystems.

Below we briefly describe the procedures of encoding and decoding which are similar to the TFM case [1]. In Fig. 4 and Fig. 5 both procedures are shown by means of an example with $m = 3$ partitioning levels.

First consider the modulation and encoding scheme (Fig. 4). The binary information sequence is divided into m binary subsequences $\underline{y}^{(j)} = (y_0^{(j)}, y_1^{(j)}, \ldots, y_n^{(j)}, \ldots)$ ($j = 1, \ldots, m$) which are separately encoded by m independent convolutional encoders. The outputs of all encoders are interleaved and then used as the m scrambler input sequences $\underline{z}^{(j)}$. The m binary output sequences $\underline{u}^{(j)}$ of the scrambler are serialized, mapped onto an M-ary sequence $\underline{u}$ with elemnts $u_n \in \{0, 1, \ldots, M-1\}$ and this is fed into the precoded GCPM modulator.

As a result of encoding and modulation, we obtain the sequence of a generalized concatenated code with inner nested MGCPM signals and outer convolutional codes.

As the jth outer convolutional code, $j = 1, 2, \ldots, m$, we use binary codes of rate R_j with parameters $(n_j, k_j, d_f^{(j)})$ and overall constraint length ν_j. where $d_f^{(j)}$ denotes the free Hamming distance.

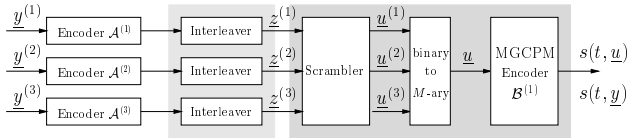

Fig. 4: Encoding and modulation scheme for GCC with 3 partitioning levels (e.g. GCC3 or GCC4 from Table 2).

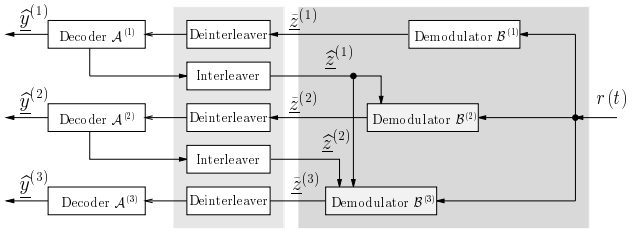

Fig. 5: Decoding and demodulation scheme for GCC with 3 partitioning levels (e.g. GCC3 or GCC4 from Table 2).

Table 2: Code rates and branch complexities for GCC constructions with MGCPM ($B_bT_s = 0.3$, $h = 1/M$).

Name of constr.	M	L	Scrambler	overall Rate R [bps]	Code Rate R_c	R_{A_1}	R_{A_2}	R_{A_3}	decoding complexity per bit	+ demod. complexity per bit	= branch complex. per bit
GCC4	8	2	I_3	$5/2$	$5/6$	$1/2$	1	1	$1/5 \cdot 32$	$2/5 \cdot (512+64+8)$	240 [a]
GCC3	8	2	I_3	2	$2/3$	$1/8$	$7/8$	1	$1/2 \cdot 32$	$1/2 \cdot (512+64+8)$	308
4GCPM	4	2	—	2	1	1	—	—	0	$1/2 \cdot 64$	32
GCC2	4	2	C_2	$4/3$	$2/3$	$1/3$	1	—	$1/4 \cdot 32$	$3/4 \cdot (64+8)$	62 [b]
GCC1	4	2	C_2	1	$1/2$	$1/14$	$13/14$	—	32	$(64+8)$	104 [c]
GMSK	2	2	—	1	1	1	—	—	0	8	8
GCCc	8 (4)	1	I_3 (I_2)	$3/2$	$1/2$	0	$1/2$	1	$1/3 \cdot 32$	$2/3 \cdot (16+4)$	24
GCCb	8 (4)	1	I_3 (I_2)	$4/3$	$4/9$	0	$1/3$	1	$1/4 \cdot 32$	$3/4 \cdot (16+4)$	23
GCCa	8 (4)	1	I_3 (I_2)	1	$1/3$	0	$1/5$	4/5	32	$(16+4)$	52

Corrections after publication in *Proc. European Wireless '99 – 4.ITG-Fachtagung "Mobile Kommunikation"*, ITG Fachbericht 157, pages 331 – 396, Munich, Germany, October 1999:

[a] Accidentally the worse value $298 = 1/5 \cdot 32 + 2/3 \cdot (512+64+8)$ was given in the published version.

[b,c] These both values had accidentally been swapped in the published version. See also discussion of simulation results (footnote 1).

The overall code rate of GCC then is

$$R_c = (1/m) \sum_{j=1}^{m} R_j$$

with $R_j = k_j/n_j$. The overall Rate (in bits per symbol, bps) of the encoded modulation scheme can be calculated as

$$R = \log_2(M) R_c \quad .$$

In case of termination of the MGCPM modulation or the outer codes there exists some fractional rate loss. This is neglected in the following as blocklengths are expected to be large enough.

Now consider the demodulation and decoding scheme (Fig. 5). The generalized concatenated decoding (GCD) algorithm of GCC also consists of m steps. Each step contains inner-stage demodulation of signals and outer-stage decoding of the convolutional codes. Consider that the signal $s(t, \underline{u})$ is transmitted, and the signal

$$r(t) = s(t, \underline{v}) + n(t)$$

is received where $n(t)$ is the additive Gaussian noise.

In the first step, i.e. $j = 1$, the received signal is demodulated on the basis of the original MGCPM trellis diagram. This procedure can be carried out by the symbol by symbol maximum *a posteriori* probability (MAP) algorithm [11] or the less complex soft-output Viterbi algorithm (SOVA) [12], which can be easily applied to CPM trellis diagrams. This results in the soft-output sequence $\underline{\tilde{z}}^{(1)} = (\tilde{z}_0^{(1)}, \tilde{z}_1^{(1)}, \dots)$ for the encoded (and interleaved) sequence $\underline{z}^{(1)}$. This is de-interleaved and used as soft-input information for the Viterbi decoder [4] of the first outer convolutional code. As a result, we obtain an information sequence $\underline{\hat{y}}^{(1)}$ and its corresponding code sequence. The interleaved code sequence $\underline{\hat{z}}^{(1)} = (\hat{z}_0^{(1)}, \hat{z}_1^{(1)}, \dots)$ uniquely defines the subtrellis that has to be used in the second step of the algorithm.

Consequently, we can demodulate the received signal again, but now according to the nested subtrellis. The result of this demodulation is the soft-output information $\underline{\tilde{z}}^{(2)}$ for the second encoded sequence and can be used as input for the second outer Viterbi decoder. This will yield a second outer information sequence $\underline{\hat{y}}^{(2)}$ and a code sequence $\underline{\hat{z}}^{(2)}$ that determines the modulation subset of the next step, and so on.

In general, at the jth step of the algorithm on the basis of the subtrellis of nested MGCPM, the received signal is demodulated, the jth outer convolutional code is decoded and the subtrellis for the $(j+1)$th demodulation step is determined.

After the demodulation and decoding of all m steps, the estimated information sequence $\underline{\hat{y}}$ is obtained by serializing the subsequences $\underline{\hat{y}}^{(1)}, \dots, \underline{\hat{y}}^{(m)}$.

The GCD algorithm can be applied both with coherent and noncoherent demodulation at the inner stage. In this paper only the case of coherent demodulation is considered.

III. Simulation Results and Discussion

In this section, we present the simulated bit error rates (BER) of generalized concatenated MGCPM based on known binary convolutional codes for the AWGN channel. We have chosen block interleavers with sizes about 1000 bits and depths of 9 to 10 rows which are sufficient to avoid the dependence of errors in the consecutive symbols of each outer code.

In order to preserve the spectral characteristics, on the transmitting side we considered MGCPM as a 4-response MCPM scheme. However, for complexity reasons, on the receiver side the MGCPM (sub)systems are demodulated on the basis of M^2-state trellis diagrams ($L = 2$). Although this is suboptimal demodulation, there is nearly no difference in bit error rate compared to optimal demodulation with $L = 4$.

Demodulation complexity increases for 8-ary MGCPM. Therefore in this case, we even used M^1-state trellis diagrams for demodulation, limiting to $L = 1$. This is real suboptimal demodulation and bit error rates deteriorate explicitly compared to optimal demodulation. Therefore different outer convolutional codes have to be chosen compared to demodulation with $L = 2$.

In the following constructions, we used MGCPM modulation with the normalized bandwidth $B_bT_s = 0.3$. We

used outer binary convolutional codes with overall constraint length $\nu_j = 4$ which have the same state complexity $W = 16$ as the 4-ary MGCPM modulation system (with $L = 2$). All code parameters were taken from [13] and [14].

For all GCC constructions presented, the parameters are listed in Table 2. We also calculated branch complexities (as proposed in [15]) and added them to Table 2.

In Fig. 6, we show the BER performance of encoded 4-ary MGCPM of rate $R = 1$ bps (GCC1) and $R = 4/3$ bps (GCC2) based on the scrambler matrix named C_2 in Table 1, and uncoded GMSK. GCC2 is constructed based on a single $(3, 1, 12)$ convolutional code. The second step remains uncoded. GCC1 is constructed based on first code $(14, 1, 56)$ and second punctured code $(14, 13, 2)$.

It can be seen, that having the same transmissioTable rate (1 bit per symbol) the rate $1/2$ encoded 4-ary MGCPM achieves a gain of approximately 4 dB at BER 10^{-5} compared to the uncoded GMSK. Branch complexity of GCC1 (104 branches[1] per information bit) is 13 times higher than that of uncoded GMSK (8 branches per information bit).

In Fig. 6, we also show the BER performance of encoded 8-ary MGCPM of rate $R = 2$ bps (GCC3) and $R = 5/2$ bps (GCC4) based on partitioning without scrambler (I_3), and uncoded 4-ary GCPM. Used code rates are given in Table 2, whereas code rate $R_j = 1$ means that some modulation step stays uncoded. It can be seen from Fig. 6, that having the same transmission rate (2 bits per symbol) the rate $2/3$ encoded 8-ary MGCPM (GCC3) achieves a gain of approximately 3 dB at BER 10^{-5} compared to the uncoded 4-ary MGCPM. Thereby branch complexity of GCC3 is about 10 times higher than that of uncoded 4-ary MGCPM.

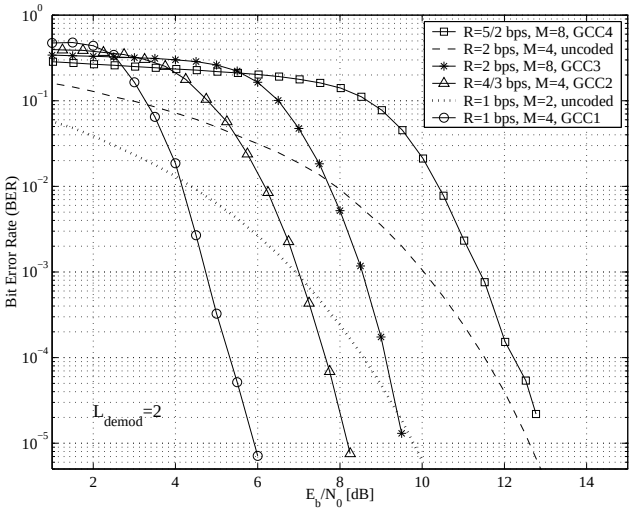

Fig. 6: Encoded 4-ary and 8-ary MGCPM with $B_bT_s = 0.3$; coherent demodulation with $L = 2$.

In addition, in Fig. 7 we show the simulation results for suboptimal demodulation with $L = 1$ of encoded 8-ary MGCPM. The results for demodulation with $L = 2$ and $L = 1$ for the case of rate $R = 1$ bps encoded 8-ary MGCPM are compared in Fig. 8.

[1]Corrected after publication. Originally the value 62 was given here, which is the branch complexity of GCC2 and only about 8 times higher than the GMSK branch complexity. See Table 2, footnote b,c.

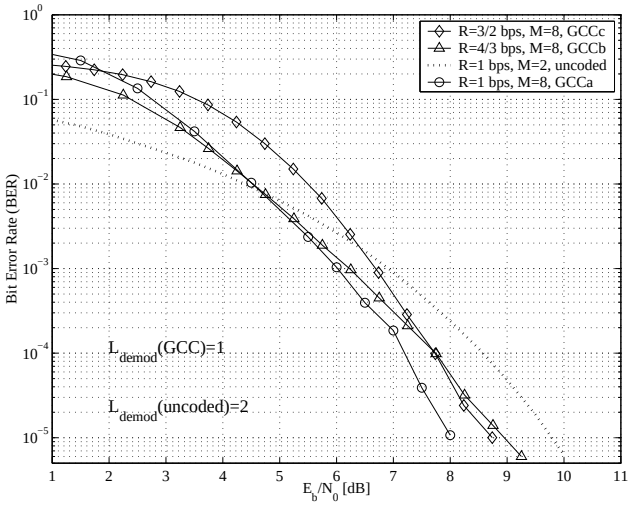

Fig. 7: Encoded 4-ary and 8-ary MGCPM with $B_bT_s = 0.3$; coherent demodulation with $L = 1$.

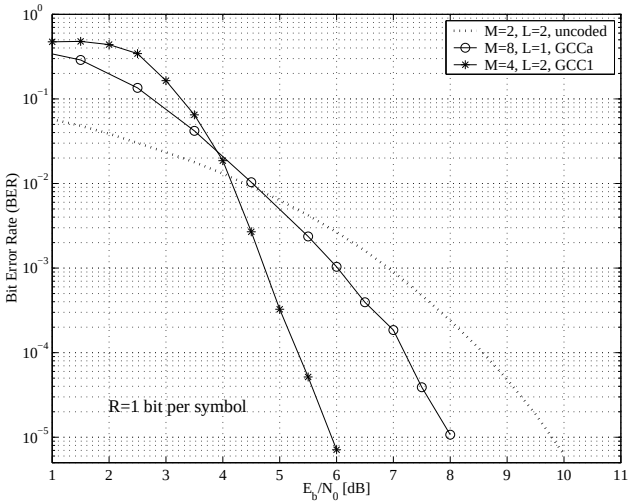

Fig. 8: Encoded 4-ary and 8-ary MGCPM with $B_bT_s = 0.3$ and rate $R = 1$ bit/symbol; coherent demodulation.

At the end, we want to point out the following advantages of encoded GCPM (and MGCPM) modulation especially with view to the EDGE project:

- As GCPM has constant envelope, no expensive linear amplifiers are needed in contrast to the proposed 8-PSK EDGE modulation. Furthermore, additional rotation of the signal is not necessary to avoid zero crossings as needed for 8-PSK modulation.
- Power estimation at the receiver is much easier (compared to the case of 8-PSK) because of the constant envelope and power of the transmitted signal.
- Because (binary) GMSK with modulation index $h = 1/2$ can be seen as a subset of M-ary GCPM with modulation index $h = 1/M$, the conventional GSM trainings sequence can be transmitted unchanged with an 8-ary GCPM modulator with $h = 1/8$. Therefore, the channel estimation can stay unchanged and no additional modifications are necessary.

- For GCPM, no additional filtering is necessary to ensure spectral efficiency as it is done in the EDGE 8-PSK proposal.
- Rate adaptation can be achieved very easily using GCC construction. For example, in case of 8-ary MGCPM, if the first partitioning step is unused (code rate $R_1 = 0$) this directly leads to 4-ary MGCPM construction with good performance for lower overall rates.

IV. REFERENCES

[1] M. Bossert, S. Shavgulidze, A. Häutle, H. Dieterich, "Generalized concatenation of encoded tamed frequency modulation," *IEEE Trans. Commun.*, vol. COM-42, pp. 1337–1345, Oct. 1998.

[2] J. B. Anderson, T. Aulin, and C.-E. Sundberg, *Digital Phase Modulation*. New York: Plenum, 1986.

[3] K. Murota and K. Hirade, "GMSK modulation for digital mobile radio telephony," *IEEE Trans. Commun*, vol. COM-29, pp. 1044–1050, July 1981.

[4] G. D. Forney, Jr., "The Viterbi algorithm," *IEEE Proc.*, vol. 61, pp. 268–278, Mar. 1973.

[5] P. Tyczka and W. Holubowicz, "Comparison of several receiver structures for trellis-coded GMSK signals: Analytical and simulation results," in *IEEE Int. Symp. on Inform. Theory*, (Ulm, Germany), p. 193, June/July 1997.

[6] B. Rimoldi, "A decomposition approach to CPM," *IEEE Trans. Inform. Theory*, vol. IT-34, pp. 260–270, Mar. 1988.

[7] A. Häutle, *Generalized Concatenation of Encoded Continuous Phase Modulation*, vol. 563 of *VDI Reihe 10*. Düsseldorf: VDI Verlag, 1998. PhD Thesis.

[8] M. Bossert, *Channel Coding for Telecommunications*. John Wiley & Sons, 1999. ISBN 0-471-98277-6.

[9] M. Bossert, H. Dieterich, and S. Shavgulidze, "Generalized concatenation of convolutional codes," *Europ. Trans. on Telecomm.*, vol. 7, pp. 483–492, Nov./Dec. 1996.

[10] M. Bossert, H. Dieterich, and S. Shavgulidze, "Partitioning of convolutional codes using a convolutional scrambler," *Electr. Letters*, vol. 32, pp. 1758–1760, Sep. 1996.

[11] L. R. Bahl, J. Cocke, F. Jelinek, and J. Raviv, "Optimal decoding of linear codes for minimizing symbol error rate," *IEEE Trans. Inform. Theory*, vol. IT-20, pp. 284–287, Mar. 1974.

[12] J. Hagenauer and P. Hoeher, "A Viterbi algorithm with soft-decision outputs and its applications," *Proc. IEEE GLOBECOM `89*, vol. 3, pp. 1680–1686, Nov. 1989.

[13] R. Palazzo Jr., "A network flow approach to convolutional codes," *IEEE Trans. Commun.*, vol. COM-43, pp. 1429–1440, Feb./Mar./April 1995.

[14] Y. Yasuda, K. Kashiki, and Y. Hirata, "High-rate punctured convolutional codes for soft decision Viterbi decoding," *IEEE Trans. Commun.*, vol. COM-32, pp. 315–319, Mar. 1984.

[15] L. F. Wei, "Trellis-coded modulation with multidimensional constellations," *IEEE Trans. Inform. Theory*, vol. IT-33, pp. 483–501, July 1987.